ELSEVIER

January 1995

Optical Materials 4 (1995) 158–162

OPTICAL Materials

Dual wavelength characterisation of shallow traps in 'blue' $BaTiO_3$

M. Kaczmarek [a,1], G.W. Ross [a], P.M. Jeffrey [a], R.W. Eason [a], P. Hribek [b], M.J. Damzen [c], R. Ramos-Garcia [c,2], R. Troth [c], M.H. Garrett [d], D. Rytz [e]

[a] *Optoelectronics Research Centre and Department of Physics, University of Southampton, Southampton SO9 5NH, UK*

[b] *Department of Physical Electronics, Faculty of Nuclear Sciences and Physical Engineering, Czech Technical University, 1519 Prague 1, Czech Republic.*

[c] *Imperial College of Science, Technology and Medicine, The Blackett Laboratory, Prince Consort Rd, London SW7 2BZ, UK*

[d] *Deltronic Crystal Industries Inc, 60 Harding Avenue, Dover NJ 07801-4710, USA*

[e] *Sandoz Huningue S.A. Centre de Recherche en Optoélectronique, Avenue de Bâle, 68330 Huningue, France*

Abstract

We report on photoinduced, intensity dependent absorption in 'blue' rhodium doped $BaTiO_3$. The change in absorption, observed under illumination by visible or infrared radiation, has successfully been modelled. Agreement obtained between theory and experiment indicates that the shallow trap model can effectively characterise the intensity dependent behaviour at red and infrared wavelength, and can be used to calculate essential photorefractive parameters in this important wavelength range for diode-laser applications.

1. Introduction

$BaTiO_3$ has always been regarded as a promising photorefractive material due to its large electrooptic coefficients and dielectric constants. However its practical applications have been impeded by its relatively long response time and limited sensitivity at near infrared wavelengths, compatible with solid state laser diodes. Research on improving the properties of $BaTiO_3$ has lead to modifications in technology of growing these crystals and using different dopants [1–3]. A new type of $BaTiO_3$ has been grown with rhodium as a main dopant, which gave the crystal a characteristic blue colour and infrared sensitivity [4]. The crystals exhibit an enhanced absorption in the red and infrared region, in comparison with a nominally undoped $BaTiO_3$, with a characteristic peak at approximately 640 nm. 'Blue' $BaTiO_3$ crystals have been also recently grown [5], by adding RhO_2 to the melt, and it has been shown that they have similar absorption characteristics and photorefractive response to the crystals reported in Ref. [4].

In this contribution we present experimental and theoretical results on intensity-dependent effects observed in 'blue' $BaTiO_3$ crystals, namely light-induced absorption and transparency [6]. We demonstrate that the 'standard model' with a single deep trap level, successfully used to describe the behaviour of undoped barium titanate, cannot be used for this new type of photorefractive crystal. In order to explain the change in absorption with intensity of illumination, shallow levels had to be included in the band–transport model. The mechanism of the photorefractive effect with a

[1] On leave from the Department of Physics, A. Mickiewicz University, 60-780 Poznań, Poland.

[2] On leave from Instituto Nacional de Astrofisica, Optica y Electronica, Apdo. Postal 51 y 216, 72000 Puebla, Pue. Mexico.

SSDI 0925-3467(94)00054-9

two level system succeeded in explaining complex photorefractive phenomena such as a sublinear dependence of the response time on intensity, intensity dependent space-charge field and absorption coefficient [6–8].

The additional traps, existing closer to the valence band edge, can play a significant role in the charge distribution, mainly capturing carriers photoionised from deep traps. This important modification of the number of active photorefractive levels is particularly relevant for compatibility of 'blue' $BaTiO_3$ with longer, infrared wavelengths, since lower energy photons within this spectral region are also capable of photoexcitation.

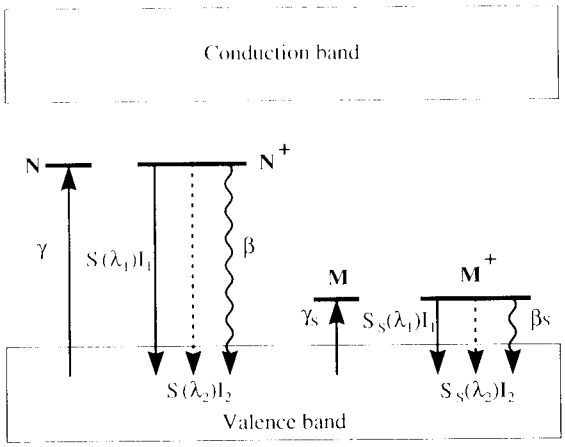

Fig. 1. Model diagram of photorefractive infrared-sensitive $BaTiO_3$ with deep and shallow centres and two wavelength illumination.

2. Theoretical framework

Light-induced absorption is commonly interpreted in terms of a two-centre model, assuming deep and shallow traps with an intensity-dependent population [6–8]. The additional secondary photorefractive centres are shallower than the primary deep centres and highly ionised at room temperature. However, when the crystal is illuminated, shallow traps acquire holes generated by photoabsorption of the deep traps. Since the photoionisation cross-sections of deep and shallow levels are different, this change in distribution of charges is reflected in the change of absorption coefficient for the illuminating light.

We used a two-centre model, hence assuming just one additional trap centre, with one dominant charge carriers, viz. holes, and considered the effect of dual wavelength illumination on the absorption. A schematic diagram of our model is presented in Fig. 1.

For hole transport in our material we consider deep 'empty' donor traps (concentration denoted by N) and 'filled', acceptor sources (concentration denoted by N^+) with total deep centre concentration $N_D = N + N^+$. M and M^+ are the concentrations of shallow centres with total shallow centre density $M_T = M + M^+$. The parameters S, β, and γ are, respectively, the cross-section for photoionisation, rate of thermal ionisation and the recombination constant. The unsubscripted parameters refer to the deep centres and the corresponding parameters with subscript 's' refer to shallow-trap coefficients. I_1 and I_2 are the intensities of beams 1 (signal) and 2 (pump), with wavelengths λ_1 and λ_2, respectively. We assume that all photons absorbed result in the photoionisation of a charge carrier, i.e. the quantum efficiencies of both deep and shallow centres are taken as unity.

The material equations derived for the two-centre model previously [7,8] have been modified to include the two wavelength illumination. Since in our case signal and pump beams are incoherent, there is no beam coupling between them. The signal beam is therefore only influenced by the presence of the second beam via an intensity dependent contribution to the thermal ionisation rates of the deep and shallow centres and given by:

$$\beta(I_2) = \beta + S(\lambda_2) I_2 , \tag{1}$$

$$\beta_s(I_2) = \beta_s + S_s(\lambda_2) I_2 , \tag{2}$$

where $S(\lambda_2)I_2$ and $S_s(\lambda_2)I_2$ are the photoionisation rates due to pump beam 2. To calculate the intensity dependence of the absorption coefficient, we assumed uniform illumination for both beams, set the electric field and current to zero in the material equations, and solved them under steady-state conditions. By doing this we obtain the following expression for the population of shallow centres filled with holes due to photoinduced transfer of charge from the deep levels [8]:

$$M^+ = \sigma(I_1, I_2)\{\xi(I_1, I_2) - [(\xi(I_1, I_2))^2 - 4\rho(I_1, I_2)(\rho(I_1, I_2) - 1) N_D M_T]^{1/2}\} , \tag{3}$$

where

$$\rho(I_1, I_2) = \frac{\gamma_s S(\lambda_1)}{\gamma S_s(\lambda_1)} \left(\frac{1 + \beta(I_2)/S(\lambda_1) I_1}{1 + \beta_s(I_2)/S_s(\lambda_1) I_1} \right), \quad (4)$$

$$\sigma = \frac{1}{2(\rho(I_1, I_2) - 1)}, \quad (5)$$

and

$$\xi = \rho(I_1, I_2)\,(N_D + M_T) + N_D - N_A\,. \quad (6)$$

N_A is the concentration of compensating acceptors.

Note that Eq. (4) reduces to Eq. (10) in Ref. [8] in the case of a single beam I_1 and low thermal ionisation rate β of deep centres.

The redistribution of charge between deep and shallow centres causes a change in the absorption coefficient of the crystal proportional to M^+ as given by Eq. (3). So the absorption coefficient at wavelength λ_1 due to the presence of both beams is given then by the formula:

$$\alpha(I_1, I_2) = (hc/\lambda_1)\{S(\lambda_1) N_A + [S_s(\lambda_1) - S(\lambda_1)]\, M^+(I_1, I_2)\}, \quad (7)$$

and $\alpha_0 = (hc/\lambda_1)\, S(\lambda_1)\, N_A$ is the low intensity absorption coefficient, when $I_1 = I_2 \simeq 0$, assuming all the absorption is associated with the deep centre photorefractive species N^+ ($= N_A$ in the dark). Note that α increases if $S_s(\lambda_1) > S(\lambda_1)$ (induced absorption) and decreases if $S_s(\lambda_1) < S(\lambda_1)$ (induced transparency). Fig. 2 is a plot of M^+ (according to Eqs. (3) to (6)) normalized to the total number of shallow centres M_T as a function of illumination intensity I_1 at different intensities of beam I_2. The curves are based on the crystal parameters given in Table 1, with signal beam 1 corresponding to wavelength 633 nm and pump beam 2 to wavelength 800 nm. As we can see, the density of filled shallow traps is a saturating function of the intensity I_1. The bold line corresponds to $I_2 = 0$ and, as we can see in this case, at low intensity the density of filled shallow centres M^+ is only weakly populated because the thermal ionisation rate from the shallow centres dominates over the transfer of charge from the deep centres by photoexcitation from beam 1. As the intensity I_1 increases the photoexcitation dominates over the thermal excitation and therefore a significant filling of the shallow traps is obtained.

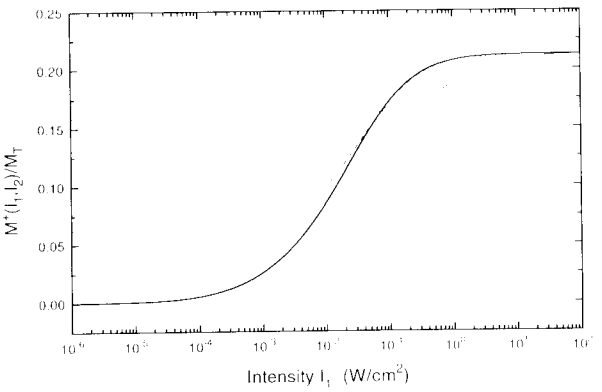

Fig. 2. Theoretical plot of the density of filled shallow centres normalised to the total density of shallow centres as a function of the intensity I_1 at different intensities of beam 2: $I_2 = 0$ (bold line), $I_2 = 10$ mW/cm^2 (dashed line), $I_2 = 100$ mW/cm^2 (dotted line) and $I_2 = 1$ W/cm^2 (solid line).

If the thermal ionisation rate from deep traps is negligible and $I_2 = 0$, Eq. (4) shows that strong intensity-induced filling of the shallow centres occurs at a characteristic saturation intensity given by $I_1 = I_{sat} = \beta_s/S_s(\lambda_1)$ [8,11]. This intensity corresponds approximately to the region of the inflexion point in the curve in Fig. 2. A redefinition of the saturation intensity is needed when the shallow illumination source is included, as described by Eqs. (1) and (2). It is seen in Fig. 2 that at high values of I_1 the maximum amount of filling of the shallow traps is independent of I_2, and its dependence is only through the ratio $\rho_0 = [\gamma_s S(\lambda_1)]/[\gamma S_s(\lambda_1)]$, which is the saturated value of the parameter ρ given by Eq. (4.) If $\rho_0 \ll 1$, the shallow traps are weakly populated, and if $\rho_0 \gg 1$ they are almost completely populated. It is noted that at a particular intensity $I_1 = I_0$, the density of filled shallow traps remains constant, regardless of the magnitude of the secondary beam I_2 as shown by the common crossing point of the curves in Fig. 2. From Eq. 4 it is found that the particular intensity I_0 can be expressed as:

$$I_0 = I_{sat} \left(\frac{1 - \eta I_D/I_{sat}}{\eta - 1} \right), \quad (8)$$

where

$$I_D = \beta/S(\lambda_1), \quad \text{and}$$

$$\eta = [S_s(\lambda_2) S(\lambda_1)]/[S_s(\lambda_1) S(\lambda_2)].$$

Physically, the crossing point only occurs when $\eta > 1$. In most of the photorefractive crystals the dark (ther-

Table 1
Crystal parameters used in numerical simulations

	Deep centres	Secondary centres
Density of species	$N_D = N + N^+ = 1.3 \times 10^{18}$ cm^{-3}	$M_T = M + M^+ = 1.1 \times 10^{18}$ cm^{-3}
	$N_{dark} = N_D - N_A = 2 \times 10^{16}$ cm^{-3}	$M^+_{dark} = 0$
Photoexcitation cross-section at 633 nm	$S = 13.4$ cm^{2}J^{-1}	$S_s = 2$ cm^{2}J^{-1}
Photoexcitation cross-section at 800 nm	$S = 5.7$ cm^{2}J^{-1}	$S_s = 2.2$ cm^{2}J^{-1}
Photoexcitation cross-section at 750 nm	$S = 7.7$ cm^{2}J^{-1}	$S_s = 2.4$ cm^{2}J^{-1}
Photoexcitation cross-section at 514 nm	$S = 8.3$ cm^{2}J^{-1}	$S_s = 1.8$ cm^{2}J^{-1}
Thermal excitation rate	$\beta = 5 \times 10^{-4}$ s^{-1}	$\beta_s = 0.1$ s^{-1}
Recombination coefficient ratio γ_s/γ	0.5	0.5

mal) decay time (τ) of the charges in the deep traps is quite large and can range from several minutes to years, in particular in our crystal $\tau \sim 30$ min. Assuming $\beta \sim \tau^{-1}$, the parameter I_D is negligible and in this case, Eq. (8) reduces to $I_0 = I_{sat}/(\eta - 1)$.

3. Comparison between the numerical model and experiments

We have performed a number of photoinduced absorption measurements using both visible (514.5 and 633 nm) and infrared radiation (800 nm) [12]. We observed light-induced transparency (maximum change $\Delta\alpha = -0.55$ cm^{-1}) when an o-polarised He-Ne beam was incident on a $7.3 \times 5.6 \times 3.0$ mm^3 'blue' $BaTiO_3$ crystal. However, the transmission characteristics for this beam were significantly changed when a second, strong pump beam (also o-polarised) from a Ti:sapphire laser was simultaneously incident onto the crystal. In this case the absorption increased by up to 0.2 cm^{-1} for an incident infrared beam of 10 W/cm^2. The experimental results obtained for absorption dependence on different intensities and for different wavelengths, were then interpreted using the theoretical model described earlier. In order to determine the essential parameters required for modelling, additional experiments on two-beam coupling and dark decays had to be performed [12] yielding important information such as effective trap density, and thermal excitation rates of shallow traps. Using these parameters, we have determined values for the photoionisation cross-section of $S_s \sim 2$ cm^2 J^{-1} at 633 nm, and a total density of shallow traps $M_T \sim 1.1 \times 10^{18}$ cm^{-3}. Once the shallow trap properties have been characterised at a certain wavelength, we are able to determine the magnitudes of photoionisation cross-section at any other wavelength, using the absorption spectrum and by fitting the change in the absorption coefficient to experimental data. The model parameters used in our theoretical fits to experimental data are summarised in Table 1.

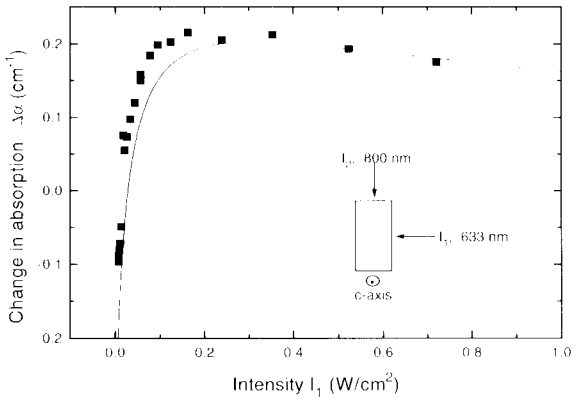

Fig. 3. Change in the absorption coefficient at 633 nm as a function of the He-Ne intensity I_1 with and without I_2 (800 nm); $I_2 = 1.3$ W/cm^2. Filled dots are experimental data taken as shown in inset, solid line is a theoretical curve based on the parameters given in Table 1.

Fig. 3 presents the experimental data and the theoretical fit for the change of absorption for an o-polarised He-Ne beam ($\lambda = 633$ nm) in the presence of an o-polarised $\lambda_2 = 800$ nm beam. The o-polarised beams were used in order to minimise photorefractive grating effects and errors due to fanning. The intensity of the secondary illuminating beam I_2 was kept constant at 1.3 W/cm^2 and the transmission of the He-Ne beam was monitored as a function of intensity with and without beam I_2. The change in absorption co-

efficient according to Eq. (7) can now be written as $\Delta\alpha(I_1) = \alpha(I_1, I_2 = 1.3\ \mathrm{W/cm^2}) - \alpha(I_1, 0)$. It may be noted from Fig. 3 that the theoretical prediction (plotted as a solid line) reproduces the experimental results quite well. Similar agreement was achieved for other Ti:sapphire infrared wavelengths [12].

We have also conducted experiments at other wavelengths to extend our model to the visible (green) spectral region. Fig. 4 is a plot of the change of the absorption coefficient for He-Ne (633 nm) with a pump beam of wavelength 514.5 nm, and intensity $I_2 = 3.6\ \mathrm{W/cm^2}$: $\Delta\alpha(I_1) = \alpha(I_1, I_2 = 3.6\ \mathrm{W/cm^2}) - \alpha(I_1, 0)$.

To produce the theoretical curves we used the same numerical model with the parameters predicted for 514.5 nm, as given in Table 1. As can be seen the agreement between theory and experiment presented in Fig. 4 is also good. Residual discrepancies may indicate that we have reached the limits of the two-centre model, and in order to obtain better results other effects such as inclusion of electrons as well as holes, participating in the charge transport, or more complicated trap-level structures will have to be tested. In fact, it has been recently suggested that the three-trap level model, with a third centre in the middle of the gap is able to reproduce accurately the change of absorption occurring at visible wavelengths [13].

4. Conclusions

We have performed dual-wavelength intensity-dependent absorption measurements in 'blue' $BaTiO_3$ using simultaneous visible and infrared radiation. In parallel, a theoretical model was derived to aid the interpretation of the experimental results and to identify, and quantify, deep and shallow trap parameters. We have shown that the band-transport model which includes shallow traps adequately explains the observed change in absorption for different wavelengths. Additionally, we have provided a method to control the absorption coefficient by simultaneous illumination with two beams of different wavelengths. Extension of this model to incorporate more than two traps may prove to be necessary to simulate results obtained with shorter wavelength visible radiation. However, such an approach may encounter similar difficulties through further unknown parameters for any additional traps invoked.

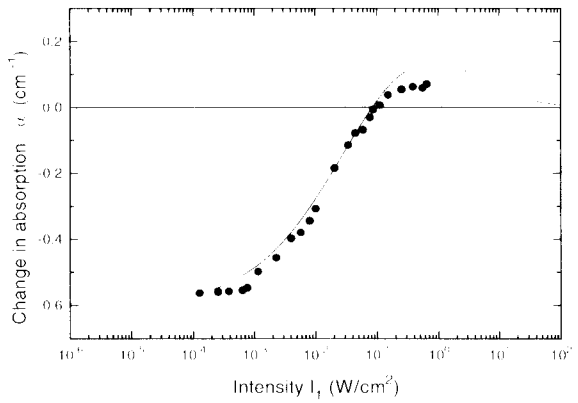

Fig. 4. Change in the absorption coefficient at 633 nm as a function of the He-Ne intensity I_1 with and without I_2 (514.5 nm); $I_2 = 3.6\mathrm{W/cm^2}$. Filled dots are experimental data, solid line is a theoretical curve based on the parameters given in Table 1.

References

[1] D. Rytz, B.A. Wechsler, M.H. Garrett, C.C. Nelson, R.N. Schwartz, J. Opt. Soc. Am. B 7 (1990) 2245.
[2] D. Rytz, R.R. Stephens, B.A. Wechsler, M.S. Keirstead, T.M. Baer, Optics Lett. 15 (1990) 1279.
[3] M.H. Garrett, J.Y. Chang, H.P. Jenssen, C. Warde, Optics Lett. 17 (1992) 103.
[4] G.W. Ross, P. Hribek, R.W. Eason, M.H. Garrett, D. Rytz, Optics Comm. 101 (1993) 60;
C. Warde, T.W. McNamara, M.H. Garrett, P. Tayebati, SPIE Conference, San Diego, CA, CR48-07, July 1993;
T.W. McNamara, S.G. Conahan, I. Mnushkina, M.H. Garrett, H.P. Jenssen, C. Warde, SPIE Critical Review Proceedings, Vol. CR-48, eds. P. Yeh, C. Gu (1994).
[5] B.A. Wechsler, M.B. Klein, C.C. Nelson, R.N. Schwartz, Optics Lett. 19 (1994) 536.
[6] G.A. Brost, R.A. Motes, J.R. Rotgé, J. Opt. Soc. Am. B 5 (1988) 1879.
[7] L. Holtmann, Phys. Stat. Sol. (A) 113 (1989) K89.
[8] P. Tayebati, D. Mahgerefteh, J. Opt. Soc. Am. B 8 (1991) 1053.
[9] G.A. Brost, R.A. Motes, Optics Lett. 15 (1990) 538.
[10] R.A. Motes, G.A. Brost, J.R. Rotgé, J.J. Kim, Optics Lett. 13 (1988) 509.
[11] D. Mahgerefteh, J. Feinberg, Phys. Rev. Lett. 64 (1990) 2195.
[12] G.W. Ross, R.W. Eason, M.J. Damzen, R. Ramos-Garcia, R.C. Troth, M.H. Garrett, D. Rytz, Optics Lett., submitted.
[13] S. MacCormack, D. Berry, J. Feinberg, private communication.